Hindawi
Advances in Condensed Matter Physics
Volume 2018, Article ID 7256162, 6 pages
https://doi.org/10.1155/2018/7256162

Research Article

60GHz Reverse Modulation Fiber-Wireless System with Two Jointed DSP Algorithms

Long Chen, Ziwei He, Lv Zhao, and Bin Zhong

School of Information and Electrical Engineering, Hunan University of Science and Technology, Xiangtan 411201, China

Correspondence should be addressed to Long Chen; cl-th@163.com

Received 15 June 2018; Accepted 27 September 2018; Published 1 November 2018

Guest Editor: Qinghua Guo

In this paper, we propose a reverse modulation fiber-wireless system with two jointed DSP algorithms. The signal in the system is OFDM modulated millimeter wave (mm-wave) at 60GHz. In order to improve transmission of this system, the discrete Fourier transform spread (DFT-Spread) technology and the averaging of the channel frequency response (H-averaging) technology are applied. The DFT-Spread technology helps to reduce the peak-to-average power ratio (PAPR) of the OFDM signal, and the H-averaging technology helps to optimize channel estimation. This is the first time that the two kinds of technology were used together in this reverse modulation system. According to the simulation, the 22Gbit/s 16QAM-OFDM at 60GHz can be generated and transmitted for 90km fiber transmission under the soft decision forward error correction (SD-FEC) threshold 3.8×10^{-3}. The results show that the two jointed DSP algorithms can improve the reverse modulation system transmission performance obviously.

1. Introduction

In recent years, data flow of mobile Internet has increased quickly. Wireless and broadband communications have been the interests of the information industry. Radio-over-Fiber (RoF) technology takes advantages of the optical communication and the wireless communication to realize ultrawideband signal wireless access [1–4]. Because of high spectrum efficiency and anti-interference ability, the orthogonal frequency division multiplexing (OFDM) technology is intensively studied among researchers. It is widely accepted that OFDM technology in RoF system helps millimeter wave signal to resist the dispersion effect in optical link and multipath fading during the wireless transmission. It is also considered as an effective solution in the future wireless access [5–7]. Many countries have opened the frequency spectrum resources around 60GHz for free, which attracts many companies and teams to undertake research [8–10]. To solve the problems which limit the performance of the RoF system, a novel reverse modulation system which is energy efficient, dispersion free, and data format compatible has been proposed [11].

The reverse modulation system with OFDM signal transmission has got more and more attention and studies since it was proposed [12, 13]. However, there are still many problems that need to be solved. The high PAPR will influence some devices such as the amplifier in mm-wave system. Therefore, the PAPR needs to be reduced to enhance the transmission quality. Besides, the OFDM signal in reverse modulation system will be interfered by noises caused by optical channel and wireless channel, so it is vital to estimate the channel estimation correctly. When it comes to the aforementioned problems, digital signal processing could be taken into consideration.

This paper proposed an OFDM modulated mm-wave at 60GHz reverse modulation system based on cascaded advanced digital signal processing algorithms. The H-averaging is used in the system to optimize channel estimation and the DFT-Spread is used to reduce the PAPR. Simulation results show that the performance of the reverse modulation system has been significantly improved with application of the H-averaging technology and the DFT-Spread technology. This is the first time that the two advanced

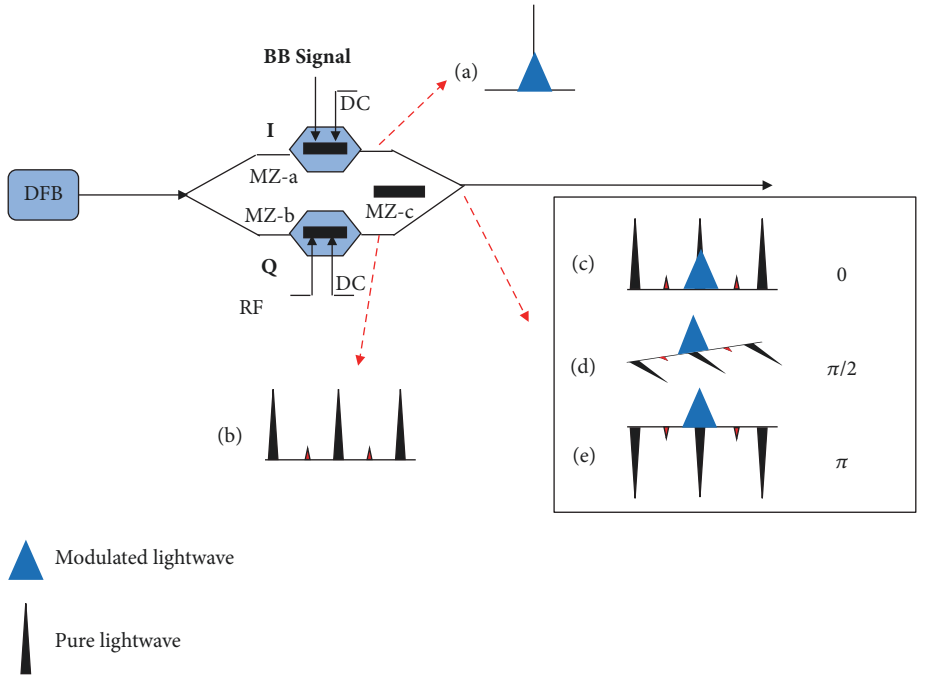

Figure 1: Principle of parallel Mach-Zehnder modulator.

digital signal processing algorithms have been cascaded in the reverse modulation system.

2. Principle of Reverse Modulation System with Jointed DSP Algorithms

The tandem SSB (TSSB) system is intensively studied [14, 15] for its frequency doubling effect in the optical domain. Compared to the TSSB, the reverse modulation system can eliminate the electrical mixer whose imperfect features such as nonlinearity, bandwidth limitation, and conversion loss will limit system performance seriously. Furthermore, the reverse modulation system is energy efficient and dispersion robust [12]. The reverse modulation system is based on a parallel Mach-Zehnder modulator (P-MZM) which is shown in Figure 1. The lightwave is split into two paths: MZ-a at the up path and MZ-b at the down path. The MZ-a is driven by the baseband data and its optical spectrum is illustrated in Figure 1(a). The MZ-b is driven by electrical LO to generate optical millimeter wave, and its DC-bias is driven at the top point of its transfer curve. Figure 1(b) is the optical spectrum of signal from MZ-b. Then optical signals from two branches are coupled in MZ-c at the end of P-MZM and their schematic optical spectra are illustrated in Figures 1(c)-1(e). By adjusting the bias voltage of MZ-c, the phase difference between the two optical signals is changed. As shown in Figure 1(e), when the phase difference is set to be 180°, the optical direct current component will be suppressed due to the interference between the two optical signals. The data is carried by the alternative current component which means that the modulation power efficiency will be improved when the phase difference is close to 180°. Thus, the modulation power efficiency can be changed by the MZ-c and be max when the phase difference is 180°.

One major drawback of the OFDM technology is that the modulated signal has a high PAPR. When the instantaneous power of the OFDM signal is too large, the gain of the amplifier in the system tends to be saturated at that time. Nonlinear distortion may be caused because the OFDM signal is clipped. In the RoF systems especially the reverse modulation system, nonlinearity also exists in the fiber transmission, so reducing the impact of the PAPR is a challenge for the designed system. The DFT-Spread technology can be used to reduce the PAPR of the OFDM signal, so that multicarrier modulated OFDM signal can show the characteristics of single-carrier modulated signals [16]. Figure 2 shows the principle of the DFT-Spread OFDM signal generation and recovery. Compared with the conventional OFDM signal, the DFT-Spread scheme performs the DFT of the K point and zero symbols inserted before the IDFT. The data expand into a new sequence of N points after the zero symbols inserted and go through the IDFT. Other processes are the same as the conventional OFDM modulation. In addition, one more IDFT process is performed when OFDM signal demodulation is performed at the demodulation.

In the reverse modulation system, receiving noise created by detector through photon-electrical conversion greatly affects the system performance. However, the H-averaging technology can improve the accuracy of channel estimation by suppressing receiving noise [17]. In OFDM systems, training sequence is often used to estimate the frequency response of the channel. The H-averaging is that, in a training sequence period, the channel response H_k of the k-th subcarrier is known to be adjacent to the first m subcarriers and the last m subcarriers. The channel response value is averaged, and

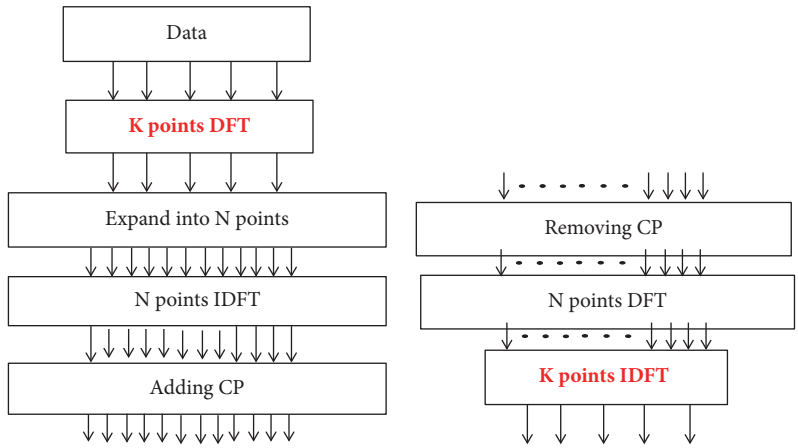

(a) DFT-SOFDM modulation (b) DFT-S OFDM demodulation

Figure 2: Principle of the DFT-Spread OFDM signal generation and recovery.

the calculated optimal channel response value for the k-th subcarrier is as follows.

$$H_{ISFA} = \frac{\sum_{k'=k-m}^{k+m} H_{k'}}{\min\left(k'_{\max}, k+m\right) - \max\left(k'_{\min}, k-m\right) + 1} \quad (1)$$

The $k'_{\max}$ and $k'_{\min}$ represent the largest and the smallest subcarrier numbers, respectively. When the subcarrier index is beyond the range between the minimum and maximum subcarrier numbers, the value of the channel response is 0. The optimized channel response value can be used to recover the received signal. The number of averaged subcarriers used in calculating the channel response for each subcarrier is called tap size, which affects the performance of H-averaging technology. The average number of subcarrier samples will be larger when the tap size increases, which is more conducive to suppress random noise. However, if the number is too large, the correlation between the subcarrier samples may be weakened, so the accuracy of channel estimation may be affected. Therefore, choosing the optimal tap size needs to get a balance between the suppression of random noise and the correlation between subcarriers.

3. Simulation Results

In this section, the simulation platform will be set up to verify the designed system and also to investigate the performance influenced by the two jointed DSP algorithms. The simulation setup will be described with key parameters. Results from simulations will be described and analyzed. The simulation system diagram is shown in Figure 3. The modulation and demodulation process of the baseband OFDM signal is performed offline in the Matlab software. The data transmitted in this simulation is firstly mapped into the 16QAM format. Each OFDM symbol includes 200 data subcarriers which carry data information. 56 null subcarriers are inserted for the guard interval, and the cyclic prefix of 32 subcarriers is provided to reduce intercarrier interference and intersymbol interference, so there are a total of 288 subcarriers per symbol period. Then the digital OFDM baseband signal becomes an electrical signal through a digital-to-analog converter (DAC) in the system, and a low pass filter (LPF) removes middle and high order band and noise. The lightwave with a center frequency of 193.1THz is generated from a distributed feedback (DFB) laser. The power of the lightwave is 10dBm and the linewidth is 10MHz. With bandwidth of 8GHz, the electrical OFDM baseband signal is sent into the MZM-a, and the MZM-a works in the linear region. The local radio frequency at 30GHz is sent into the MZM-b to drive the DC offset at the highest point of its modulation curve, and the odd numbered sideband is suppressed. The optical signal is coupled in the phase MZM-c after coming out of the MZM-a and MZM-b, and the modulation power efficiency is controlled by adjusting the phase deviation in the MZM-c. The output signal is amplified by an optical amplifier before being transmitted into a standard single-mode fiber (SSMF). In all the simulation test examples, the power of the signal before entering the fiber is 0 dBm. An optical amplifier is then used to compensate for the loss of the signal after passing through the optical link. A rectangular optical bandpass filter is used to filter out unwanted sidebands. After filtering, the light signal is then detected by a photo detector (PD). The detected electrical signal goes through a rectangular band pass filter (EBPF) with a center frequency of 60GHz and a bandwidth of 16 GHz. The test examples all use an electrical amplifier (EA) to amplify the power to -14dBm. Then, the generated 60GHz millimeter wave electrical signal and a signal with frequency at 60GHz from local oscillator are downconverted in an electric mixer. A LPF with bandwidth of 8GHz is used to obtain the OFDM baseband signal. The obtained OFDM baseband signal then passes through an analog-to-digital converter (ADC) into the Matlab software for further processing to test the performance of the system.

The conventional OFDM signal and the DFT-Spread OFDM signal are shown in Figure 4. Figures 4(a) and 4(b) show that the power of the DFT-Spread signal is more evenly spread comparing to that of the conventional OFDM signal. Figures 4(c) and 4(d) show the demodulation

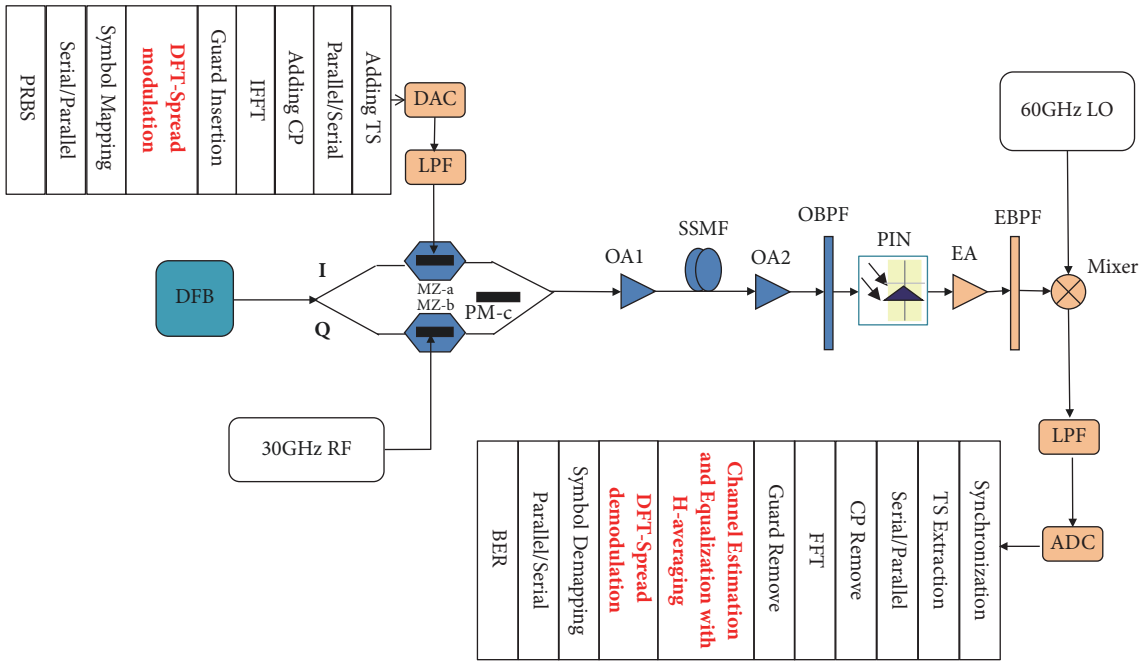

Figure 3: Simulation setup for 60GHz reverse modulation scheme.

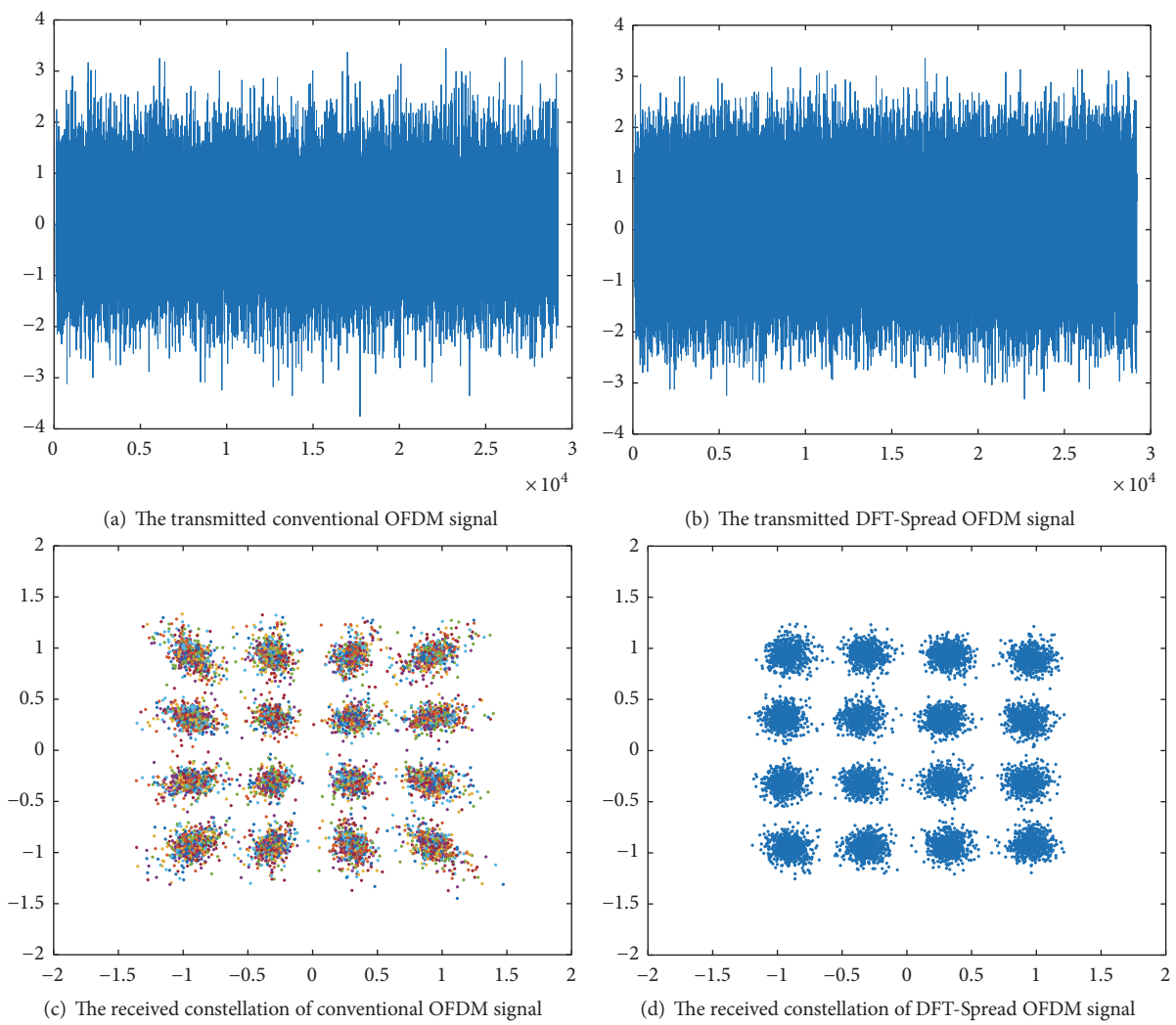

(a) The transmitted conventional OFDM signal

(b) The transmitted DFT-Spread OFDM signal

(c) The received constellation of conventional OFDM signal

(d) The received constellation of DFT-Spread OFDM signal

Figure 4: The conventional OFDM signal and the DFT-Spread OFDM signal.

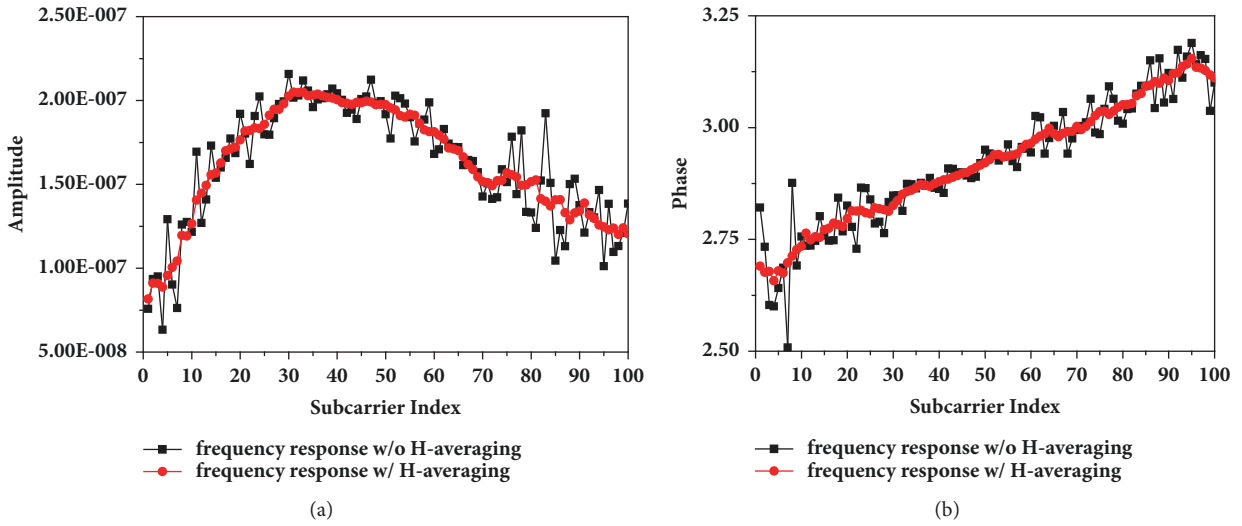

Figure 5: The channel frequency response curves of OFDM signal.

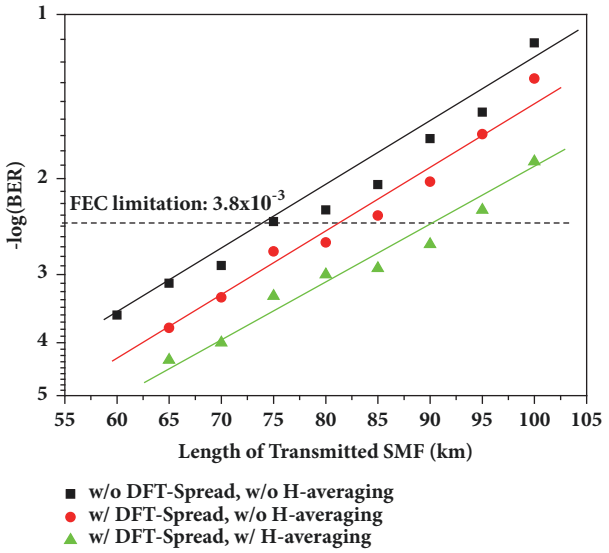

Figure 6: BER versus distances with different algorithms.

constellation of the received conventional OFDM and DFT-Spread OFDM signal after 65km fiber transmission. We can see that the received constellation of DFT-Spread signal converges more. Compared to the conventional OFDM, DFT-S OFDM scheme contains one more DFT operation in the signal modulation and one more IDFT in the signal demodulation. DFT-Spread technique can make the OFDM signal with multicarrier modulation have the characteristic of single-carrier signal, and mitigate the fiber nonlinearity. The transmission quality of DFT-Spread OFDM signal in the system is obviously better than that of conventional OFDM signal.

Figure 5 shows the channel frequency responses of the subcarriers in OFDM signal. A training sequence used for channel estimation is inserted at the front of data frames in every 100 OFDM symbols. The channel response curves obtained by training sequences in different frames are different. However, in every 100 OFDM frames, we assume the channel responses of the OFDM frames are the same as the channel responses of the adjacent training sequence. The result shows the channel responses of the following 100 OFDM frames. By suppressing the noise, the frequency response curves with the H-averaging are relatively flat compared to the curves without the H-averaging. There is a tradeoff in choosing the tap size. The tap size should be large for noise suppression while the taps number should not be too large for channel estimation accuracy. The BER measured in the system is the minimum when the optimal tap size is 4.

We obtain the bit error rate (BER) curves versus length of transmitted single-mode fiber in Figure 6. The mm-wave at 60GHz is generated in the system. The transmitted OFDM signal carried by the mm-wave has 8GHz bandwidth, and the total rate is 22Gbit/s. In the simulation, the phase difference between the optical signals is adjusted to be 180°, so that the modulation power efficiency is the maximum. The optimal tap size used in the H-averaging technology is 4. In the simulation, 22Gbit/s 16QAM DFT-Spread OFDM signal was successfully transmitted for 90km fiber when BER is controlled at the SD-FEC threshold where the redundancy is 7% (the bit error rate is 3.8×10^{-3}). The result shows that the system with the DFT-Spread technology can transmit the DFT-Spread OFDM signal over about 10km fiber distance more than the conventional OFDM signal. By reducing the PAPR and suppressing the in-band noise, the system with two jointed DSP algorithms can transmit the signal over more than 15km fiber distance compared to the system without any DSP algorithms.

4. Conclusions

This paper proposed a reverse modulation fiber-wireless system with two jointed DSP algorithms. The DFT-Spread and the H-averaging technology are applied for improving

the transmission performance. In the simulation, the mm-wave at 60GHz carrying 16QAM-OFDM signal with 22Gb/s rate is generated and transmitted in the optical link. The BER of the generated signal after 90km optical link can be controlled within the SD-FEC threshold. The results show that DFT-Spread and the H-averaging technology can improve the reverse modulation system transmission performance by more than 15km fiber transmission at the SD-FEC threshold 3.8×10^{-3}.

Data Availability

The data used to support the findings of this study are available at https://pan.baidu.com/s/1F_1LX2uZs9n3ilWjXKtQ2w. The key of the webpage is b3vi.

Conflicts of Interest

The authors declare that there are no conflicts of interest regarding the publication of this paper.

Acknowledgments

This paper is supported by the National Natural Science Foundation of China (U1501253, 61875054) and the Scientific Research Startup Foundation for Doctor of the Hunan University of Science and Technology (E51862).

References

[1] X. Li and J. Yu, "2 × 2 multiple-input multiple-output optical-wireless integration system based on optical independent-sideband modulation enabled by an in-phase/quadrature modulator," *Optics Expresss*, vol. 41, no. 13, pp. 3138–3141, 2016.

[2] T. Umezawa, A. Kanno, K. Kashima et al., "Bias-free operational UTC-PD above 110 GHz and its application to high baud rate fixed-fiber communication and W-band photonic wireless communication," *Journal of Lightwave Technology*, vol. 34, no. 13, pp. 3138–3147, 2016.

[3] J. Xiao, J. Yu, X. Li, Y. Xu, Z. Zhang, and L. Chen, "40-Gb/s PDM-QPSK signal transmission over 160-m wireless distance at W-band," *Optics Expresss*, vol. 40, no. 6, pp. 998–1001, 2015.

[4] J. Yu and L. Chen, "Phase Factor Optimization for QPSK Signals Generated from MZM Based on Optical Carrier Suppression," *IEEE Photonics Journal*, vol. 9, no. 2, pp. 1–6, 2017.

[5] C. H. Yeh, C. W. Chow, H. Y. Chen, and J. Y. Sung, "Hybrid OFDM-based multi-band wireless and baseband signal transmission in PON access," *IEEE Electronics Letters*, vol. 48, no. 7, pp. 390–392, 2012.

[6] L. Deng, X. Pang, I. T. Monroy, M. Tang, P. Shum, and D. Liu, "Experimental demonstration of nonlinearity and phase noise tolerant 16-QAM OFDM W-band (75-110 GHz) signal over fiber system," *Journal of Lightwave Technology*, vol. 32, no. 8, pp. 1442–1448, 2014.

[7] C. Tan, X. Fu, Y. Hu et al., "Plasma optical modulation for lasers based on the plasma induced by femtosecond pulses," *Optics Express*, vol. 25, no. 13, pp. 14065–14076, 2017.

[8] C.-T. Lin, C.-C. Wei, and M.-I. Chao, "Phase noise suppression of optical OFDM signals in 60-GHz RoF transmission system," *Optics Express*, vol. 19, no. 11, pp. 10423–10428, 2011.

[9] W.-J. Jiang, C.-T. Lin, A. Ng'Oma et al., "Simple 14-Gb/s short-range radio-over-fiber system employing a single-electrode MZM for 60-GHz wireless applications," *Journal of Lightwave Technology*, vol. 28, no. 16, pp. 2238–2246, 2010.

[10] F. Li, J. Yu, Z. Cao, J. Xiao, H. Chen, and L. Chen, "Reducing the peak-to-average power ratio with companding transform coding in 60 GHz OFDM-ROF systems," *Journal of Optical Communications and Networking*, vol. 4, no. 3, pp. 202–209, 2012.

[11] Z. Cao, J. Yu, L. Chen, and Q. Shu, "Reversely modulated optical single sideband scheme and its application in a 60-GHz full duplex ROF system," *IEEE Photonics Technology Letters*, vol. 24, no. 10, pp. 827–829, 2012.

[12] Z. Cao, J. Yu, F. Li et al., "Energy efficient and transparent platform for optical wireless networks based on reverse modulation," *IEEE Journal on Selected Areas in Communications*, vol. 31, no. 12, pp. 804–814, 2013.

[13] L. Chen, J. He, Y. Liu, L. Chen, and Z. Cao, "Comparison of interpolation algorithms for pilot-aided estimation of orthogonal frequency division multiplexing transmission in reversely modulated optical single sideband system," *Optical Engineering*, vol. 53, no. 5, p. 056108, 2014.

[14] P.-T. Shih, C.-T. Lin, W.-J. Jiang, Y.-H. Chen, J. Chen, and S. Chi, "Full duplex 60-GHz RoF link employing tandem single sideband modulation scheme and high spectral efficiency modulation format," *Optics Express*, vol. 17, no. 22, pp. 19501–19508, 2009.

[15] P. Gamage, A. Nirmalathas, C. Lim, D. Novak, and R. Waterhouse, "Optical tandem single-sideband-based WDM interface for millimeter-wave fiber-radio multisector antenna base station," *IEEE Transactions on Microwave Theory and Techniques*, vol. 57, no. 3, pp. 725–732, 2009.

[16] C. Li, Q. Yang, T. Jiang et al., "Investigation of coherent optical multiband DFT-S OFDM in long haul transmission," *IEEE Photonics Technology Letters*, vol. 24, no. 19, pp. 1704–1707, 2012.

[17] Q. Yang, N. Kaneda, X. Liu, and W. Shieh, "Demonstration of frequency-domain averaging based channel estimation for 40-Gb/s CO-OFDM with high PMD," *IEEE Photonics Technology Letters*, vol. 21, no. 20, pp. 1544–1546, 2009.